

Intracranial brain parenchymal spread of mucormycosis through olfactory tract: a diffusion-weighted imaging-based concept

Acta Radiologica Open
9(12) 1–5
© The Foundation Acta
Radiologica 2020
Article reuse guidelines:
sagepub.com/journals-permissions
DOI: 10.1177/2058460120980999
journals.sagepub.com/home/arr



J. Sandron , Ph. Hantson  and T. Duprez

Abstract

Mucormycosis is an opportunistic fungal infection involving among others the paranasal sinuses, nasal fossa and brain parenchyma. Mucor can invade the brain parenchyma by either contiguous spread from the paranasal sinuses or through vascular invasion. We report a case of fatal rhino-cerebral mucormycosis in whom cytotoxic edema at magnetic resonance diffusion-weighted imaging was symmetrically restricted to both neocortical and paleocortical primary areas of olfactory projection at earliest phase of the disease process. Shortly later tissue damage extended into the whole brain. This undescribed observation raised the hypothesis of preferential way of brain invasion by Mucor through the olfactory tract.

Keywords

Magnetic resonance imaging, diffusion-weighted imaging, brain, mucormycosis, olfactory tract

Received 19 August 2020; accepted 25 November 2020

Introduction

Mucormycosis is an opportunistic infection caused by fungi in the order of Mucorales. Various species in Mucor, Rhizopus, Absidia, and Cunninghamella genera are most often implicated in different clinical forms of pulmonary, gastrointestinal, cutaneous, encephalic, and rhino-cerebral infections. The cerebral angioinvasive capability of the mucormycosis has been demonstrated which leads to direct brain vessels infiltration and subsequent thrombotic occlusions. We hereby present a fatal rhino-cerebral mucormycosis infection in an immunocompromised patient who underwent serial brain MR examinations including diffusion-weighted (DW) imaging. Cytotoxic edema involving both neocortical and paleocortical primary areas of olfactory projection was observed at the earliest phase of the disease preceding devastating whole brain tissue injury.

Case history

A 42-year-old woman with end stage renal failure (ESRF) due to chemotherapy for metastatic neuroblastoma in

childhood had a second renal transplantation. An abscess in surgical wound led to a septic shock for which she was admitted to the intensive care unit (ICU) four days after surgery. Three days after admission to ICU she complained of headache and clinical examination revealed ophthalmoplegia. Head and paranasal sinus CT examination demonstrated sphenoid sinus mucosal thickening containing hyperdense so-called “Fungal balls” (Fig. 1 (a)). There was no bone destruction of orbits or olfactory grooves (Fig. 1(b)). Nasal endoscopy revealed presence of fungal hyphae embedded in the nasal mucosa, and laboratory tests of biopsy specimen confirmed presence of mucormycosis. Cerebro-spinal fluid (CSF) analysis at the time was unremarkable. Clinical worsening with increased headaches and divergent strabismus led to

Department of Neuroradiology, Clinique Universitaire St-Luc, Bruxelles, Belgium

Corresponding author:

J. Sandron, Cliniques Universitaires Saint-Luc, Avenue Hippocrate 10, Bruxelles 1200, Belgium.
Email: juliensandron@gmail.com



perform an initial MR examination the next day. The imaging protocol included diffusion-weighted (DW) sequence which failed to reveal brain parenchymal involvement (Fig. 2(a)). As the clinical status worsened in spite of initiation of standard antifungal treatment combining liposomal Amphotericin B and voriconazole, she had follow-up MR examination four



Fig. 1. CT scanner after ICU admission. (a) Transverse section in soft tissue window demonstrates hyperdense fungal ball (arrow) embedded within mucosal thickening filling the sphenoid sinus. (b) Coronal reformat in bone window demonstrates normal bone edges of olfactory grooves (arrows) and mucosal thickening in right anterior ethmoid air cells.

days later. Symmetrical areas of cytotoxic edema appeared on DW images within gyrus rectus and orbital gyrus where neocortical areas of olfactory projections are located (Fig. 2(b)). Five days later she had a third MR examination because of vision loss which revealed additional involvement of mesial temporal areas where primary paleocortical olfactory projections are located (Fig. 2(c)). The patient died a few days later. Necropsy was refused by patient's family and by pathologist because the cause of death was evident.

Discussion

Mucormycosis is a severe fungal infection affecting immunocompromised individuals. The risks factors for developing mucormycosis infection are diabetic ketoacidosis, hematologic malignancies, transplantation, corticosteroid therapy and iron overload therapy.^{1,2}

Three potential ways of intracranial spread by mucor have been suggested:

- Direct extension from nasosinusal cavities to the endocranium through osteolytic defects in the base of the skull.
- Perivascular extension across the cribriform plate of ethmoid bone to frontal lobes or through the orbital apex to the cavernous sinuses.
- Hematogenous spread from arterial wall invasion leading to occlusive downstream ischemic damage and/or abscesses.

The skull base appeared unaffected in our patient on both CT and MR images at earliest phase, as were orbital contents and cavernous sinuses (Fig. 1(b)). Direct extension through bone destruction was excluded and occurs only in late stages of the disease process.^{2,3}

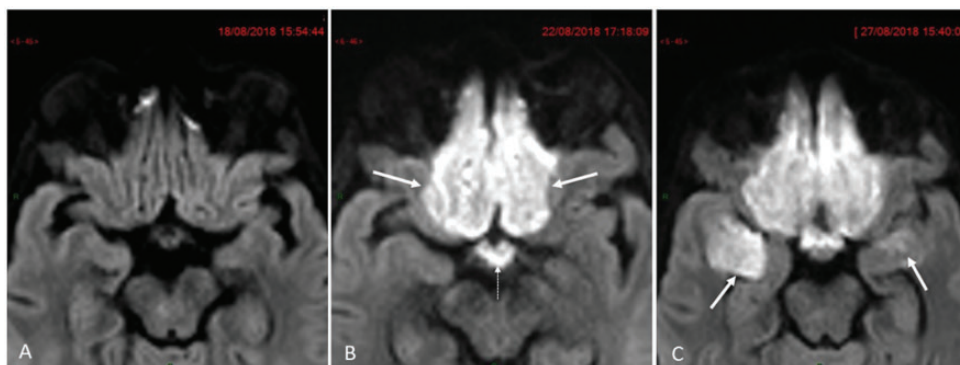


Fig. 2. Transverse diffusion-weighted (DW) magnified images in similar slice location focused on olfactory neocortical and paleocortical projection areas. (a) Unremarkable initial examination. (b) Follow-up examination four days later reveals symmetrical cytotoxic edema within primary neocortical olfactory projection areas (arrows) together with hypothalamic-optic tract (dotted arrow). (c) Repeat MRI nine days later reveals additional involvement of both temporal amygdala (arrows) which are one of the paleocortical olfactory projection areas.

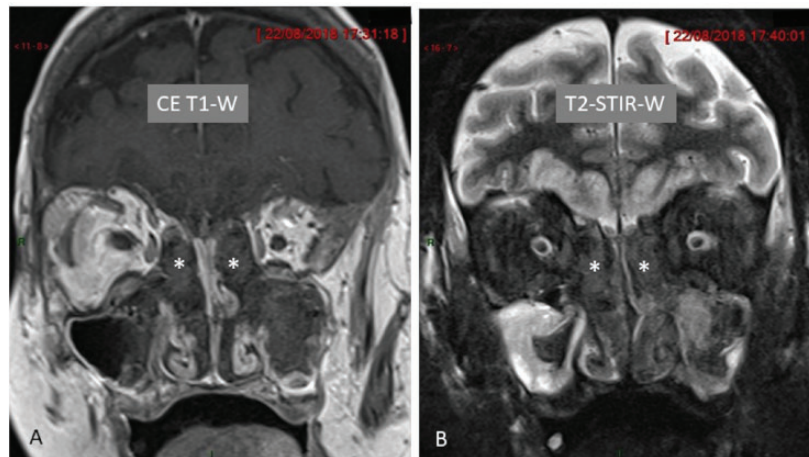


Fig. 3. Coronal post-contrast T1-W and T2-W images of paranasal sinus and nasal fossa. (a) Contrast-enhanced image demonstrates marked hypointensity of fungal material filling bilateral anterior ethmoid air cells (asterisk). (b) Coronal STIR image demonstrates marked hypointensity of fungal material (asterisk) in both anterior ethmoid air cells. In addition, there is mucosal thickening in both maxillary antrum.

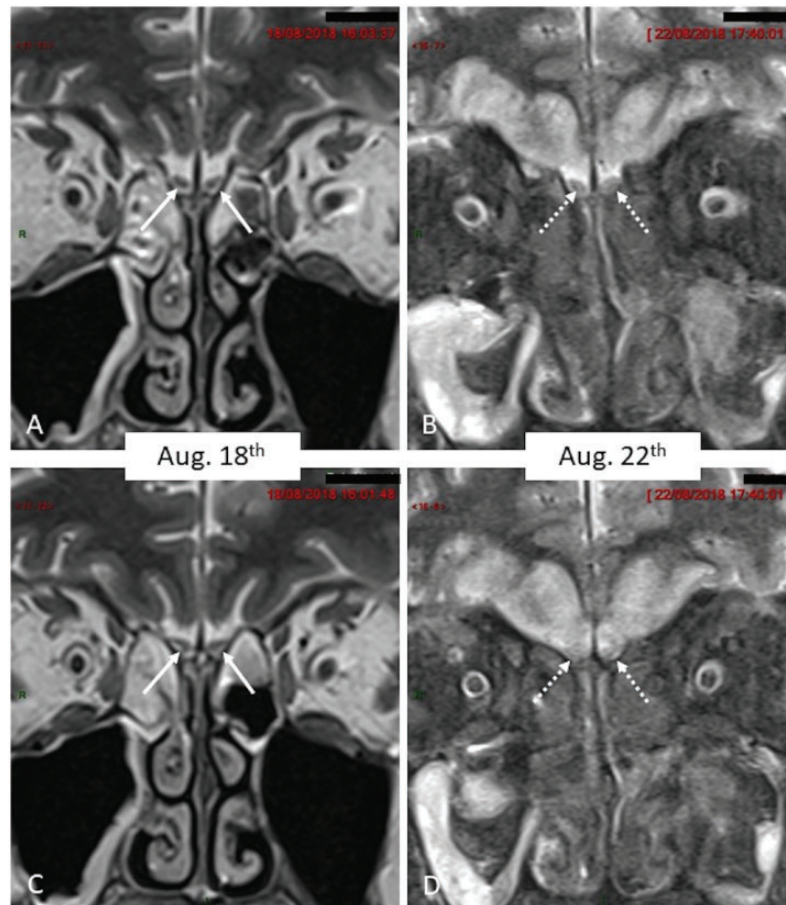


Fig. 4. Coronal T2 W magnified images of olfactory grooves. (a) Normal sized olfactory bulbs (arrows) on initial examination displaying normal hypointense signal. Only hyperintense fluid is seen within ethmoids. (b) Coronal T2-W image of olfactory grooves in similar slice location as Fig. 3(a) four days later demonstrates swelling and increased signal intensity of the olfactory bulbs (dotted arrow) together with filling of the nasal cavity by marked hypointense material (the 'black turbinate sign'). In addition, there is hyperintense signal in bilateral gyrus rectus and orbital gyrus due to spread of mucormycosis. (c) Similar findings as in Fig. 3(a) and more posterior plane (Olfactory bulbs marked by arrows). (d) Similar slice location as Fig. 3(c) demonstrates swelling and hyperintense signal within olfactory bulbs (dotted arrows).

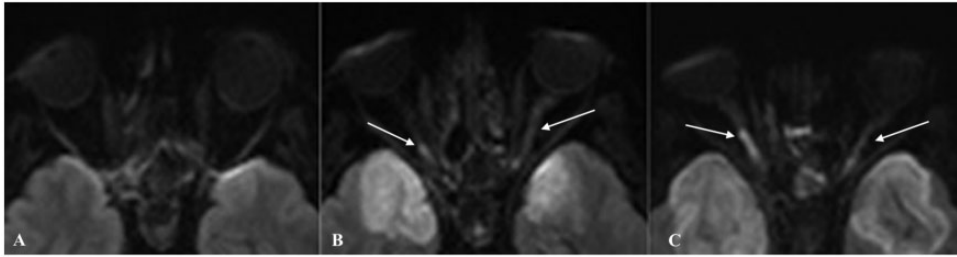


Fig. 5. Transverse diffusion-weighted (DW) demonstrates involvement of cranial nerve II. (a) Unremarkable initial examination. (b) Follow-up examination four days later reveals involvement of optic nerves bilaterally. (c) Follow-up examination nine days later reveals worsening optic nerve involvement.

Olfaction is the only sensory modality that projects to both paleocortical and neocortical areas.⁴ This unique anatomical feature had major impact on the interpretation of the MR monitoring of our patient.^{5,6} Cytotoxic edema within the brain parenchyma on DW images was the only feature in second MR examination which affected orbital gyrus and gyrus rectus which are neocortical areas of olfactory projections to which pair of medial olfactory striae abut (Fig. 2(b)). The strict symmetry and homogeneity of frontal lobe parenchymal injury on both sides and absence of true arterial territorial delineation were not consistent with hematogenous spread of infection. MR angiography was attempted but the study was suboptimal due to motion artefacts.

The third MR examination revealed further extension of the cytotoxic brain injury to the paleocortical mesial-temporal primary areas of olfactory projections (Fig. 2(c)) where the lateral olfactory striae abuts thereby giving a strong indicator that inflammation had preferentially followed the olfactory tract before further intracranial spread occurred.

Coronal MRI views illustrated the almost pathognomonic features for fungal infection of deep hypointense intensity on both T1- and T2-weighted views without contrast-enhancement (Figure 3) of the septic material filling the cavities.⁷ Moreover, olfactory bulbs invasion was evidenced by swelling and decreased T2-signal intensity of the bulbs (Fig. 4(b) and (d)).

Ophthalmoplegia and blindness resulted from contiguous invasion of the optic nerve,⁸ by true micropermeative defects through the sphenoid bone allowing early invasion of the orbital apex and cavernous sinus as highlighted by a recent review paper.⁹ The phenomenon was assessed on DW images in three serial MR examinations (Fig. 5).

Such elective and functional tract-specific way of progression cannot be explained by mere bilateral perivascular extension across cribriform plate of ethmoid. We therefore hypothesized an alternative pathophysiological mechanism of propagation: *Mucor* could have followed neuron-to-neuron extension along the

olfactory tract, mimicking what has been experimentally demonstrated for the human coronavirus OC43 in an animal model.^{10–12} Could have the hyphae of the Mucorales species a similar affinity for the olfactory neurons as shown for the human coronavirus?

In conclusion, the ability of the diffusion-weighting to track *Mucor* extension along olfactory tract could have resulted from a cytotoxic effect of the toxins released by the fungus instead of ischemic oxygen/glucose deprivation.


Declaration of Conflicting Interests


The author(s) declared no potential conflicts of interest with respect to the research, authorship, and/or publication of this article.

Funding

The author(s) received no financial support for the research, authorship, and/or publication of this article.

ORCID iDs

J. Sandron  <https://orcid.org/0000-0001-5926-1932>

Ph. Hantson  <https://orcid.org/0000-0003-4409-3352>

References

1. Cornely OA, Alastruey-Izquierdo A, Arenz D, et al. Global guideline for the diagnosis and management of mucormycosis: an initiative of the European Confederation of Medical Mycology in cooperation with the Mycoses Study Group Education and Research Consortium. *Lancet Infect Dis* 2019;19:e405–e421.
2. Petrikkos G, Skiada A, Lortholary O, et al. Epidemiology and clinical manifestations of mucormycosis. *Clin Infect Dis* 2012;54:23–34.
3. Galletti B, Gazia F, Galletti C, et al. Rhinocerebral mucormycosis with dissemination to pontine area in a diabetic patient: treatment and management. *Clin Case Rep* 2019;7:1382–1387.
4. Duprez TP and Rombaux P. Imaging the olfactory tract (cranial nerve #1). *Eur J Radiol* 2010;74:288–298.
5. Huart C, Meusel T, Gerber J, et al. The depth of the olfactory sulcus is an indicator of congenital anosmia. *AJNR Am J Neuroradiol* 2011;32:1911–1914.

6. Rombaux P, Grandin C and Duprez T. How to measure olfactory bulb volume and olfactory sulcus depth? *B-ENT* 2009;5:53–60.
7. Safder S, Carpenter JS, Roberts TD, et al. The “Black Turbinate” sign: an early MR imaging finding of nasal mucormycosis. *AJNR Am J Neuroradiol* 2010;31:771–774.
8. Chen IW, Lin CW. Rhino-orbital-cerebral mucormycosis. *CMAJ* 2019;191:E450.
9. M Coutel, C Huart, T Duprez, et al. Invasive fungal sinusitis with ophthalmological complications: Case series and review of the literature. *Neuro-Ophthalmology*. In press. DOI : 10.1080/01658107.2020.1779315
10. Dubé M, Le Coupanec A, Wong AHM, et al. Axonal transport enables neuron-to-neuron propagation of human coronavirus OC43. *J Virol* 2018;92:1–21.
11. Morris M, Zohrabian VM. Neuroradiologists, be mindful of the neuroinvasive potential of COVID-19. *AJNR Am J Neuroradiol* 2020;41:E37–E39.
12. Li YC, Bai WZ, Hashikawa T. The neuroinvasive potential of SARS-CoV2 may play a role in the respiratory failure of COVID-19 patients. *J Med Virol* 2020;92:552–555.